Emittance preservation of an electron beam in a loaded quasi-linear plasma wakefield

Veronica K. Berglyd Olsen* and Erik Adli
University of Oslo, Oslo, Norway

Patric Muggli
Max Planck Institute for Physics, Munich, Germany and
CERN, Geneva, Switzerland
(Dated: September 5, 2017)

We investigate beam loading and emittance preservation for a high-charge electron beam being accelerated in quasi-linear plasma wakefield driven by a short proton beam. The structure of the wakefield is similar to that of a long, modulated proton beam, such as the one being studied by AWAKE. We show that by exploiting two well known effects, full blow out of plasma electrons by the accelerated beam, and beam loading of the wake field, the electron beam can be accelerated without significant emittance growth.

I. INTRODUCTION

Beam driven plasma wakefield accelerators have the potential to offer compact linear accelerators with high energy gradients, and have been of interest for several decades [1]. A relativist beam travelling through a plasma excites a strong longitudinal e-field that can be loaded by a trailing witness beam. With optimal beam loading, increase in energy spread can be kept to a minimum. Acceleration of an electron withness beam by an electron drive beam has been demonstrated experimentally [2–4] in the past. AWAKE at CERN is a proof of concept proton driven plasma wakefield accelerator experiment [5].

A major challenge with plasma wakefield accelerators is, however, to produce an accelerated beam while keeping growth in energy spread and emittance as low as possible. In the well described linear case where the beam density n_b is much smaller than the plasma density n_0, the non-linear transverse wakefields cause emittance growth of the accelerated beam. A finite length beam will also see a transversely varying accelerating field causing increasing energy spread [6]. In the non-linear regime, where $n_b > n_0$, a bubble is formed by the transverse oscillations of the plasma electrons forming a sheet around an evacuated area leaving only ions. The ions, assumed stationary, form an ion channel creating a focusing force that varies linearly with radius. This produces an axially symmetric focusing force [7, 8].

A. Self-modulation as a Driver

A train of electron drive bunches with a separation λ_{pe} and a length $l_b \ll \lambda_{pe}$, where $\lambda_p = 2\pi c/\omega_{pe}$ and $\omega_{pe} = (n_0 e^2/m_e \epsilon_0)^{1/2}$, will produce a field E_z that increases for each drive bunch [1]. A tailing witness beam loading the peak accelerating phase of this field will gain

energy from the wakefield from all of the drive bunches. Acceleration of an electron witness beam driven by two electron drive beams was demonstrated at Brookhaven National Laboratory [9].

The energy carried by electron drive bunches used in previous experiments were typically small, on the order of 100 J, and the propagation length typically < 1 m [3, 10]. The energy of a high-charge electron beam accelerated to 1 TeV, similar to the beam in the international linear collider with $1e^{10}$ electrons, is 1.6 kJ. By using electron beams or lasers as drivers a large number of plasma stages is required. How to efficiently stage plasma accelerators is challenging without reducing the effective gradient and spoiling the beam quality [11, 12]. Proton drive beams available at CERN carry significantly more energy, 19 kJ for the SPS beam [13], allowing for longer accelerator stages. However, the SPS beam is orders of magnitude longer than the plasma wavelengths needed for such applications. This issue is resolved by letting the proton beam undergo self-modulation before injecting the witness beam into one of the buckets in the modulated structure. This self-modulation instability is caused by the transverse fields generated by the beam acting upon the beam itself, causing regions of the beam to rapidly defocus [14]. The modulation frequency is close to that of the plasma, and leaves a train of proton bunches along the beam axis with a surrounding halo.

B. AWAKE Run 2

The AWAKE experiment, currently in its first stages of operation at CERN, uses the SPS beam at 400 GeV as its driver, and a nominal plasma density 7×10^{14} cm^{-3} [13]. This plasma density corresponds to a plasma wavelength $\lambda_{pe} = 1.26$ mm. The plasma density is matched to the SPS proton beam such that $k_{pe}\sigma_x = 1$ where $k_{pe} = 2\pi/\lambda_{pe}$ is the plasma wave number. The aim of the first phase of Run 1 of the experiment is to demonstrate self-modulation of the proton beam, and in 2018 to sample the wakefield with a long electron beam. The study presented here is for Run 2 [15], which aims to

* v.k.b.olsen@cern.ch

demonstrate acceleration of a short electron beam to high energy with a minimal increase in emittance and energy spread.
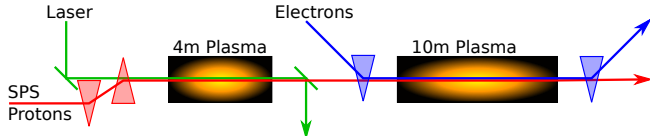

FIG. 1. A simplified illustration of the experimental setup for AWAKE Run 2. The SPS proton beam undergoes self-modulation in the first 4 m plasma cell. The electron witness beam is injected in one of the buckets, and undergoes acceleration in the second plasma cell [15, 16].

The preliminary design of the second run proposes to use two plasma sections, illustrated in figure 1. The first section of 4 m is the self-modulation stage where the proton beam undergoes self-modulation without the electron beam present. The electron witness beam will be injected into the modulated proton beam before stage two, where acceleration will occur.

With this experimental design the self-modulated proton beam does not produce a non-linear wakefield, and not all plasma electrons are therefore evacuated. The result is that the focusing force will not increase linearly with radius. The small size of the accelerating structure produced by the self-modulated beam also put constraints on the size of the electron witness beam, and thus its charge and current, if we wish to prevent large energy spread. By matching the transverse size to a practical emittance and the plasma density, we prevent large amplitude oscillations which may cause additional growth in energy spread as well as in emittance.

The key idea in this paper is that while the proton beam wake is not fully blown-out leading to non-linear focusing forces, the electron beam, if intense enough, may load the field and at the same time create its own ion bubble. As will be shown, exploiting these two well known effect, the electron beam can be accelerated, for long distances, without significant emittance growth.

II. METHOD

The main focus of this study has been on the beam loading of the electron beam. In order to eliminate other factors that may affect this, we have tried several approaches to create a stable drive beam structure based on previous self- modulation studies.

Our first approach was to use a pre-modulated, short proton beam with similar structure to the one produced by the self-modulation of the SPS beam in AWAKE. These studies were done using the full PIC code Osiris [17] using 2D cylindrical-symmetric simulations [16, 18].

In order to study the witness beam emittance evolution we turned to the recently released open source version of QuickPIC developed by UCLA. QuickPIC is a fully relativistic 3D quasi-static PIC code [19, 20]. Since QuickPIC is a quasi-static code, it does not suffer from the numerical Cherenkov effect that full PIC codes do [21, 22], it is well suited to study emittance preservation.

A. Drive Beam Parameters

In these simulations we use a single proton drive beam that sets up a wakefield comparable to that which we expect to see from the self-modulated SPS beam in the second plasma cell of AWAKE Run 2 (Figure 1). When the initial SPS beam containing 3×10^{11} protons [13] enters the second plasma cell the peak E_z field is expected to be $500 - 600 \, \text{MV/m}$. As the baseline AWAKE drive beam current is insufficient to reach the non-linear regime and produce a plasma bubble, the plasma electrons are only depleted to around 65% of nominal plasma density at the point where we inject the electron beam [23]. These conditions are replicated in our simulations using a single proton beam of 1.46×10^{10} protons, or $2.34 \, \text{nC}$ and $7 \, \text{kA}$.

The peak density of the simulation drive beam is $0.83 \cdot n_0$, producing a quasi-linear wakefield. The single bunch setup uses the baseline proton energy $W_{pb} = 400 \, \text{GeV}$ and transverse size $\sigma_x = 200 \, \mu\text{m}$. We set the length of the drive beam to $\sigma_z = 40 \, \mu\text{m}$. In order to create a stable environment to study the evolution of the witness beam we prevented the proton beam from evolving radially by increasing the particle mass by a factor of 1e^6. We are not considering the evolution of the proton beam itself in this study.

B. Witness Beam Parameters

The witness beam in our simulation differs from AWAKE baseline parameters on several key points. Initial beam energy is set such that $\gamma_{eb} = \gamma_{pb} = 426.3$. This was done to eliminate the problem of initial de-phasing of the witness beam. Beam loading of a short witness beam is sensitive to its position relative to the field [24]. The relative drift causing the de-phasing $\Delta \xi \propto \gamma^{-2}$. By simply matching the initial γ values we eliminate this effect entirely, but a lower initial value is likely to be sufficient [16].

In these 3D simulations we have used a matched beam for an initial emittance of $2 \, \mu\text{m}$, corresponding to a σ_x of $5.25 \, \mu\text{m}$. The beam matching relation is given by

$$\beta = \frac{\sigma_r^2}{\epsilon_g} = \frac{\lambda_{pe}}{2\pi}\sqrt{2\gamma_{rel}}, \quad (1)$$

where λ_p is the plasma wavelength. This is a very narrow beam compared to the drive beam $\sigma_x = 200 \, \mu\text{m}$. The charge density of this compact witness beam reaches that of the plasma density at only a few pC, but reaches optimal beam loading at around $1 - 200 \, \text{pC}$. The implication here being that the witness beam produces its own non-linear wakefield already at the head of the beam. The

majority of the electrons within it will therefore see a linear focusing force preventing the bulk of the beam from undergoing emittance growth.

The relatively small size of the witness beam compared to the proton beam put some restrictions on the transverse resolution of the witness beam. We used a transverse grid cell size of $1.17\,\mu$m, and $2.34\,\mu$m for the longitudinal grid cells. The witness beam was simulated with 16.8 M non-weighted particles.

In the following section we study a witness beam with a total charge of $100\,$pC, a $\sigma_z = 60\,\mu$m, and with a $\sigma_x = 5.23\,\mu$m matching an initial normalised emittance $\epsilon_0 = 2\,\mu$m. We refer to this parameter set as our base case.

III. BEAM LOADING
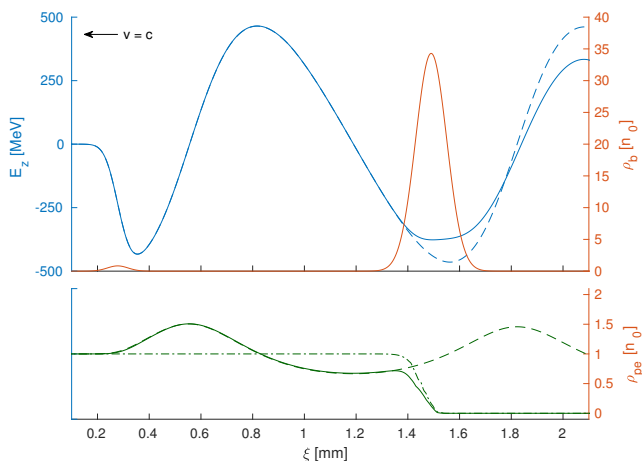
FIG. 2. The top plot compares the unloaded longitudinal e-field (no witness beam, blue. dashed line) and the loaded e-field (blue line) along the beam axis. The magnitude of the beam density along the axis is shown (red line) for reference. The bottom plot compares the plasma density along the beam axis for a drive beam with no witness beam (dashed green line), witness beam with no drive beam (dash-dotted green line), and both witness and drive beam present (continuous green line). $\xi = z - tc$ is the position in the simulation box and both beams travel towards the left. The beam and plasma densities are in units of initial plasma density $n_0 = 7 \times 10^{-14}\,$cm^{-3}.

The single drive beam setup is designed to behave similarly to the self-modulated case. However, since the drive beam is prevented from significant transverse evolution, we are presented with an idealised case where the electron witness beam sees consistent wakefields throughout the plasma stage. The E_z-field generated by the proton drive beam is seen as the blue line in figure 2, shown with and without the electron beam present. With a proton beam density $n_{pb} \simeq n_0$, we are in the quasi-linear regime but near non-linear [25]. The dashed green line in the lower part of figure 2 shows that the on-axis plasma den-
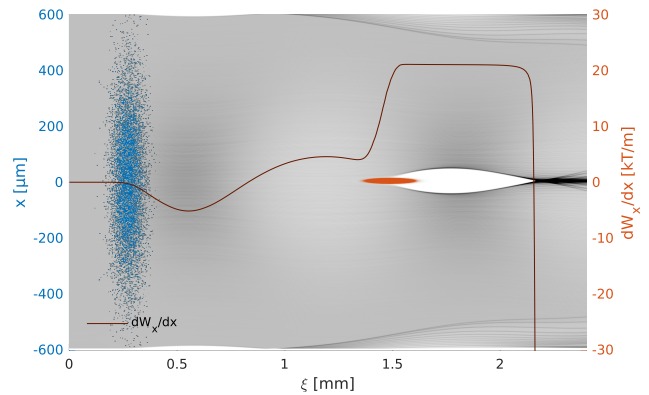

FIG. 3. The plasma density in grey with the proton beam (blue) and the electron beam (red) superimposed. The line plot indicates the transverse wakefield gradient dW_x/dx where $W_x = E_x - v_b B_y$, evaluated along the beam axis.

sity has a depletion of 67%, close to what we see in full scale reference simulations for AWAKE Run 2 [23].

The witness beam generates its own wakefield which partially cancels out the E_z field generated by the drive beam. With an ideally shaped electron beam charge profile it is possible to optimally load the field, such that the accelerating E_z is constant along the bunch [6, 24].
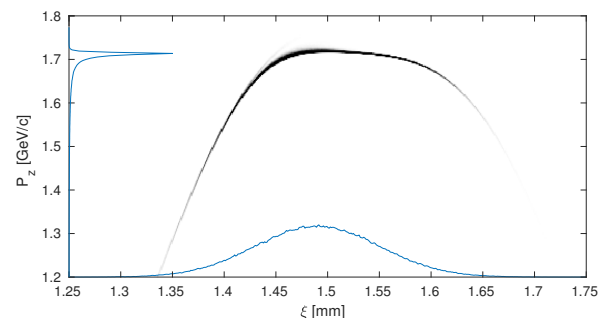

FIG. 4. Phase space charge distribution of a $100\,$pC, $60\,\mu$m long witness beam after $4\,$m of plasma. Mean momentum is $1.67\,$GeV/c with an RMS spread of $87\,$MeV/c (5.2%) for the full beam.

While the ideal shape is trapezodial, for Gaussians beams a reasonable flat field, and consequently low energy spread, can be achieved by controlling the charge density to achieve a similar effect. This, however, puts the front of the witness beam outside of the ideal region while the middle bulk of the beam has a trapezoidal-like shape. In our case, with a matched beam to the plasma density defined by equation 1, we are limited on how much total charge we can accelerate without reaching charge densities that will overload the field.

As illustrated in figure 4 our base case shows a difference in energy transfer to the tail of the beam compared to the centre where the E_z-field is nearly flat. Also the front of the beam has a large tail in momentum space
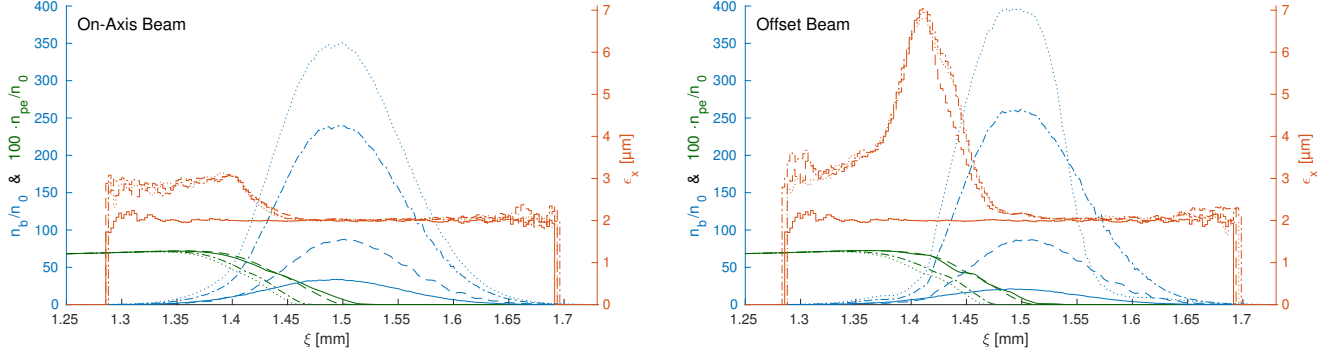
FIG. 5. The red lines show a moving window calculation of transverse normalised emittance for an on-axis beam with respect to the drive beam axis (left) and an offset beam (right) with an offset of one $\sigma_x = 5.24\,\mu$m in the x plane. The moving window for emittance calculation is longitudinal slices of $l = 4 \times \Delta\xi = 18.75\,\mu$m with a $\Delta\xi$ resolution. Only slices with more than 100 macro particles have been included, which accounts for the abrupt edge as well as the noise at either end of the beam due to low statistics. The blue lines show the peak electron beam density profile. For reference, the plasma density profile is included in green, but scaled up by a factor of 100 to be visible. The solid lines are at the plasma entry point, the dashed lines after 4 m of plasma, the dash-dotted after 40 m, and the dotted after 100 m. In order to sustain a stable accelerating field for the witness beam, these simulations were run with an LHC energy drive beam of 7 TeV to avoid de-phasing which causes the structure to break down after about 50 m.
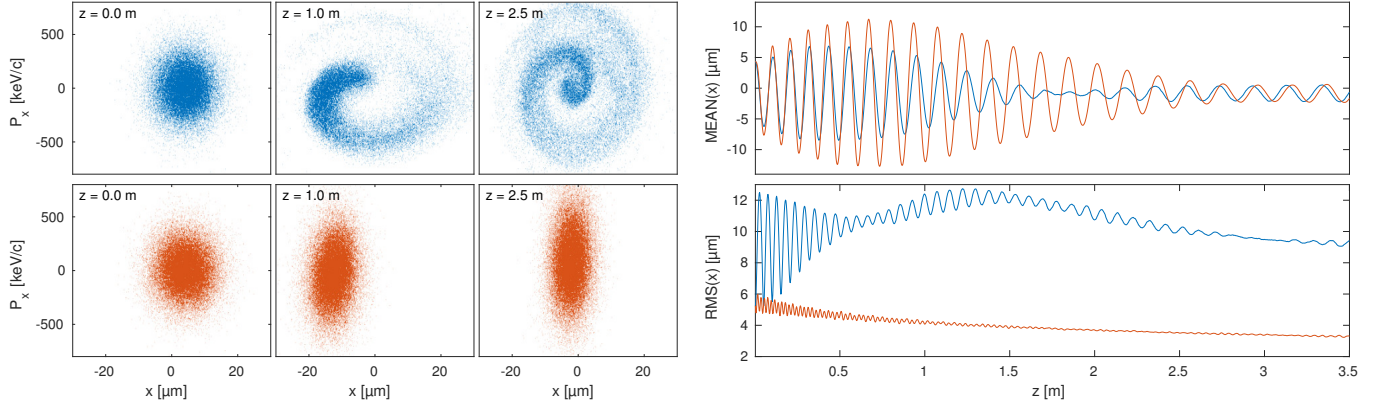

FIG. 6. The left plots show the transverse phase space of the electron beam at different plasma positions. The Right side shows the macro particle mean position (top) and RMS spread (bottom). The blue particles and lines represent particles with position $1.40\,\mu$m $< \xi < 1.42\,\mu$m. The red particles and lines represent particles with position $1.55\,\mu$m $< \xi < 1.57\,\mu$m.

as this regions sees a smaller accelerating field. The positioning of the witness beam is chosen to put the bulk of the charge as close to the peak accelerating field as possible.

The charge density required to optimally load the E_z field is $n_{eb} \approx 35 \times n_0$. This means that the witness beam's own wakefield is in the fully non-linear regime, where the space charge force is sufficient to blow-out all plasma electrons resulting in an ion column. This ion column, as is well known [26], provides a linear focusing force on the part the electron beam within the ion column, and therefore prevents emittance growth for this region. This effect is shown for our base case in figure 3. The focusing field has a gradient of 20 kT/m near the beam axis.

For the majority of the cases we studied that maintained a stable accelerating structure, about $70 - 80\%$ of

the beam retained its initial emittance. Figure 5 shows emittance growth for the base case as a function of propagation length. No significant emittance growth was observed for propagation lengths up to 100 m. The drive beam energy increased to 7 TeV (LHC energy) to prevent de-phasing. De-phasing for the SPS beam case starts to become significant after about 50 m.

The on-axis density of the electron beam increases as its gamma factor increases and its transverse size decreases. The beam radius follows the evolution given by equation 1 with $\lambda_{pe} = \lambda_0$ for the section of the beam where normalised emittance is preserved as shown in figure 6. This has the potential to cause overloading of the field. However, for our base case this effect is not significant.

Since the accelerated electron beam creates its own fo-

cusing bubble, the emittance of the part of the beam inside the bubble is not affected by small beam offsets with respect to the proton beam axis. This is an added benefit of this new accelerating regime, and may ease the transverse injection tolerances. The head of the beam does not benefit from this effect, but since the proton beam creates a quasi linear wake, the head of the beam still stabilises after some time. This is illustrated on figure 5 for an electron beam offset of $1\sigma_x$. In this case there is a larger initial emittance growth (see left hand plots of figure 6), but the emittance growth stop after the first few metres (figure 5). This effect is likely to be greater for larger offsets as the beam oscillates around the axis of the drive beam wakefield (see right hand plots of figure 6).
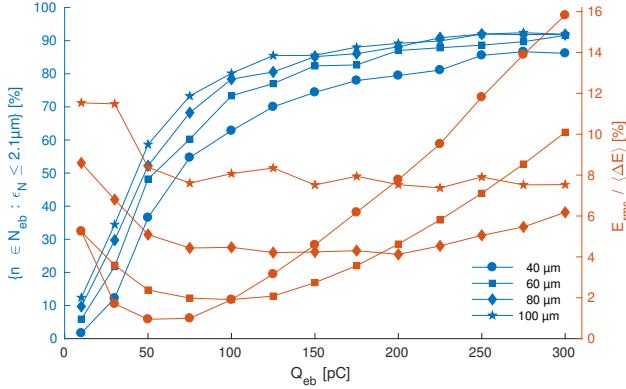
IV. PARAMETER OPTIMISATION

FIG. 7. Ratio of total beam charge with an emittance growth $\Delta\epsilon \leq 5\%$ as a function of initial beam charge (blue), and relative energy spread of the accepted charge (red), after 4 m of plasma and with an initial emittance $\epsilon_{N,0} = 2\,\mu$m. These are shown for four different σ_z from $40\,\mu$m to $100\,\mu$m. The detailed studies presented in beam loading section corrspond to the square marked lines at 100 pC.

The beam loading and blow out properties of the electron beam depends on a large number of parameters: the longitudinal profile, the transverse profile as well as the relative phasing of the proton and the electron beams.

We here study parameter optimization relevant for AWAKE Run 2, in order to understand the ideal injection parameters. For AWAKE Run 2 we desire to maximize the energy gain, minimize the energy spread, maximize the charge to be accelerated and minimize the emittance growth. In addition, the bunch length should be such that it is possible to generate and transport by a compact electron injector [15]. These are contradictory constraints. We investigate the interdependence of these parameters by simulation. We vary the electron bunch length, charge and initial emittance. We quantify the resulting emittance growth, energy spread and and energy
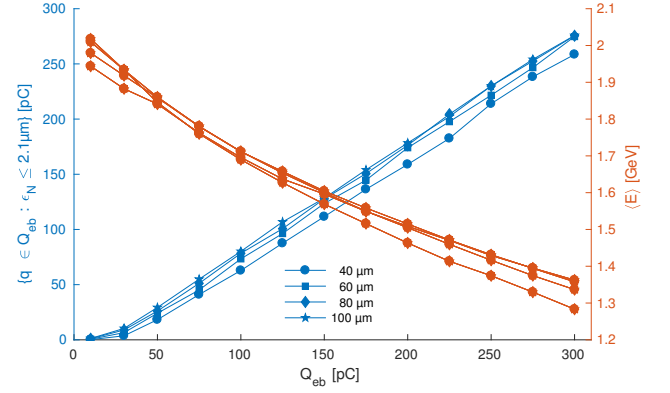
FIG. 8. Total beam charge with an emittance growth $\Delta\epsilon \leq 5\%$ as a function of initial beam charge (blue), and final momentum (red), after 4 m of plasma and with an initial emittance $\epsilon_{N,0} = 2\,\mu$m.

gain. The desired injection parameters will depend on the application.

Figures 7 and 8 show the dependence on bunch length and bunch charge for an initial beam emittance of $2\,\mu$m after propagating through 4 m of plasma. We ran the scan with beam charges from 10 pC to 300 pC and with length σ_z from $40\,\mu$m to $100\,\mu$m. We see from figure 7 that both the $40\,\mu$m and the $60\,\mu$m beam has a well defined minimum energy spread with a beam charge ≥ 50 pC and ≈ 100 pC respectively. Lower beam charges tend to underload the E_z-field, while higher beam charges tend to overload it. It is also clear that long beams with respect to the accelerating flank of the E_z-field, $\approx \lambda_{pe}/4$, will not optimally load the field along its length thus experiencing a larger spread in energy.
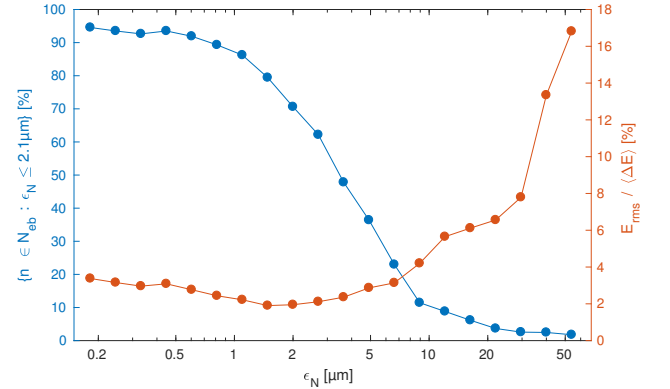
FIG. 9. Ratio of total beam charge with an emittance growth $\Delta\epsilon \leq 5\%$ as a function of initial emittance (blue), and relative energy spread of the accepted charge (red), after 4 m of plasma.

Figure 9 shows how the growth in emittance and energy spread varies with initial electron beam emittance. The smaller the initial emittance is, the better the emit-

tance is preserved. There are two effects that lead to growth for high emittance beams; the transverse beam size may increase beyond the size of the bubble, or the beam density may be reduced so much that the plasma electrons are no longer fully evacuated from the ion column. Emittance values higher than a few micrometers lead to a significant increase in both emittance and energy spread. In these simulations the focusing of the beam to the plasma remains matched for each emittance value.

V. CONCLUSION

We have studied a new plasma wakefield acceleration regime; acceleration of a strongly loaded electron beam in a quasi- linear proton driven wake. When optimally loaded, the electron beam creates its own ion bubble, yielding emittance preservation for a large parts of the electron beam.

These result indicates that emittance preservation for an on-axis injected electron beam, properly optimized, is feasible. Parameter studies indicate that up to a few $100 \, \mathrm{pC}$ might be accelerated, for bunches of length $40 - 60 \, \mu\mathrm{m}$. Such an electron bunch may be generated by a standard S-band RF gun.

As this study assumes a wake driven by a single, short proton beam, the studies for interesting cases for AWAKE should be repeated by a full simulation of a self-modulated proton beam.

VI. ACKNOWLEDGEMENTS

[1] P. Chen, J. M. Dawson, R. W. Huff, and T. Katsouleas, Physical Review Letters **54**, 693 (1985).

[2] J. B. Rosenzweig, D. B. Cline, B. Cole, H. Figueroa, W. Gai, R. Konecny, J. Norem, P. Schoessow, and J. Simpson, Physical Review Letters **61**, 98 (1988).

[3] I. Blumenfeld, C. E. Clayton, F.-J. Decker, M. J. Hogan, C. Huang, R. Ischebeck, R. Iverson, C. Joshi, T. Katsouleas, N. Kirby, W. Lu, K. A. Marsh, W. B. Mori, P. Muggli, E. Oz, R. H. Siemann, D. Walz, and M. Zhou, Nature **445**, 741 (2007).

[4] E. Kallos, T. Katsouleas, W. D. Kimura, K. Kusche, P. Muggli, I. Pavlishin, I. Pogorelsky, D. Stolyarov, and V. Yakimenko, Physical Review Letters **100**, 074802 (2008).

[5] AWAKE Collaboration, R. Assmann, R. Bingham, T. Bohl, C. Bracco, B. Buttenschn, A. Butterworth, A. Caldwell, S. Chattopadhyay, S. Cipiccia, E. Feldbaumer, R. A. Fonseca, B. Goddard, M. Gross, O. Grulke, E. Gschwendtner, J. Holloway, C. Huang, D. Jaroszynski, S. Jolly, P. Kempkes, N. Lopes, K. Lotov, J. Machacek, S. R. Mandry, J. W. McKenzie, M. Meddahi, B. L. Militsyn, N. Moschuering, P. Muggli, Z. Najmudin, T. C. Q. Noakes, P. A. Norreys, E. z, A. Pardons, A. Petrenko, A. Pukhov, K. Rieger, O. Reimann, H. Ruhl, E. Shaposhnikova, L. O. Silva, A. Sosedkin, R. Tarkeshian, R. M. G. N. Trines, T. Tckmantel, J. Vieira, H. Vincke, M. Wing, and G. Xia, Plasma Physics and Controlled Fusion **56**, 084013 (2014).

[6] T. Katsouleas, S. Wilks, P. Chen, J. M. Dawson, and J. J. Su, Particle Accelerators **22**, 81 (1987).

[7] W. Lu, C. Huang, M. Zhou, W. B. Mori, and T. Katsouleas, Physical Review Letters **96**, 165002 (2006).

[8] W. Lu, C. Huang, M. Zhou, M. Tzoufras, F. S. Tsung, W. B. Mori, and T. Katsouleas, Physics of Plasmas (1994-present) **13**, 056709 (2006).

[9] P. Muggli, B. Allen, Y. Fang, V. Yakimenko, M. Fedurin, K. Kusche, M. Babzien, C. Swinson, and R. Malone, in Proceedings of PAC2011 (New York, NY, USA, 2011) pp. 712–714.

[10] A. Caldwell, K. Lotov, A. Pukhov, and F. Simon, Nature Physics **5**, 363 (2009).

[11] S. Steinke, J. van Tilborg, C. Benedetti, C. G. R. Geddes, C. B. Schroeder, J. Daniels, K. K. Swanson, A. J. Gonsalves, K. Nakamura, N. H. Matlis, B. H. Shaw, E. Esarey, and W. P. Leemans, Nature **530**, 190 (2016).

[12] C. A. Lindstrom, E. Adli, J. M. Allen, J. P. Delahaye, M. J. Hogan, C. Joshi, P. Muggli, T. O. Raubenheimer, and V. Yakimenko, Nuclear Instruments and Methods in Physics Research Section A **829**, 224 (2016).

[13] E. Gschwendtner, E. Adli, L. Amorim, R. Apsimon, R. Assmann, A. M. Bachmann, F. Batsch, J. Bauche, V. K. Berglyd Olsen, M. Bernardini, R. Bingham, B. Biskup, T. Bohl, C. Bracco, P. N. Burrows, G. Burt, B. Buttenschn, A. Butterworth, A. Caldwell, M. Cascella, E. Chevallay, S. Cipiccia, H. Damerau, L. Deacon, P. Dirksen, S. Doebert, U. Dorda, J. Farmer, V. Fedosseev, E. Feldbaumer, R. Fiorito, R. Fonseca, F. Friebel, A. A. Gorn, O. Grulke, J. Hansen, C. Hessler, W. Hofle, J. Holloway, M. Hther, D. Jaroszynski, L. Jensen, S. Jolly, A. Joulaei, M. Kasim, F. Keeble, Y. Li, S. Liu, N. Lopes, K. V. Lotov, S. Mandry, R. Martorelli, M. Martyanov, S. Mazzoni, O. Mete, V. A. Mi-

nakov, J. Mitchell, J. Moody, P. Muggli, Z. Najmudin, P. Norreys, E. z, A. Pardons, K. Pepitone, A. Petrenko, G. Plyushchev, A. Pukhov, K. Rieger, H. Ruhl, F. Salveter, N. Savard, J. Schmidt, A. Seryi, E. Shaposhnikova, Z. M. Sheng, P. Sherwood, L. Silva, L. Soby, A. P. Sosedkin, R. I. Spitsyn, R. Trines, P. V. Tuev, M. Turner, V. Verzilov, J. Vieira, H. Vincke, Y. Wei, C. P. Welsch, M. Wing, G. Xia, and H. Zhang, Nuclear Instruments and Methods in Physics Research Section A **829**, 76 (2016).

[14] N. Kumar, A. Pukhov, and K. Lotov, Physical Review Letters **104**, 255003 (2010).

[15] E. Adli and AWAKE Collaboration, in *Proceedings of IPAC 2016*, International Particle Accelerator Conference (JACoW, Busan, Korea, 2016) pp. 2557–2560.

[16] V. K. Berglyd Olsen, E. Adli, P. Muggli, L. D. Amorim, and J. Vieira, in *Proceedings of IPAC 2015* (Richmond, VA, USA, 2015) pp. 2551–2554.

[17] R. A. Fonseca, L. O. Silva, F. S. Tsung, V. K. Decyk, W. Lu, C. Ren, W. B. Mori, S. Deng, S. Lee, T. Katsouleas, and J. C. Adam, in *Computational Science ICCS 2002*, Lecture Notes in Computer Science No. 2331, edited by P. M. A. Sloot, A. G. Hoekstra, C. J. K. Tan, and J. J. Dongarra (Springer Berlin Heidelberg, 2002) pp. 342–351.

[18] V. K. Berglyd Olsen, E. Adli, P. Muggli, and J. Vieira, in *Proceedings of NAPAC 2016* (Chicago, IL, USA, 2016).

[19] C. Huang, V. K. Decyk, C. Ren, M. Zhou, W. Lu, W. B. Mori, J. H. Cooley, T. M. Antonsen, and T. Katsouleas, Journal of Computational Physics **217**, 658 (2006).

[20] W. An, V. K. Decyk, W. B. Mori, and T. M. Antonsen, Journal of Computational Physics **250**, 165 (2013).

[21] B. B. Godfrey, Journal of Computational Physics **15**, 504 (1974).

[22] R. Lehe, A. Lifschitz, C. Thaury, V. Malka, and X. Davoine, Physical Review Special Topics - Accelerators and Beams **16**, 021301 (2013).

[23] AWAKE Collaboration and A. Caldwell, *AWAKE Status Report, 2016*, Tech. Rep. CERN-SPSC-2016-033 (CERN, Geneva, 2016).

[24] M. Tzoufras, W. Lu, F. S. Tsung, C. Huang, W. B. Mori, T. Katsouleas, J. Vieira, R. A. Fonseca, and L. O. Silva, Physics of Plasmas **16**, 056705 (2009).

[25] J. B. Rosenzweig, G. Andonian, M. Ferrario, P. Muggli, O. Williams, V. Yakimenko, and K. Xuan, AIP Conference Proceedings **1299**, 500 (2010).

[26] J. B. Rosenzweig, B. Breizman, T. Katsouleas, and J. J. Su, Physical Review A **44**, R6189 (1991).